Electric Field-Induced Functional Reductions in the K^+ Channels Mainly Resulted from Supramembrane Potential-Mediated Electroconformational Changes

Wei Chen,* Yu Han,* Yan Chen,* and Dean Astumian#
*Departments of Dermatology and Physiology and Biophysics, The University of Illinois at Chicago, Chicago, Illinois 60612, and #Department of Plastic and Reconstructive Surgery, The University of Chicago, Chicago, Illinois 60637 USA

ABSTRACT The goal of this study is to distinguish the supramembrane potential difference-induced electroconformational changes from the huge transmembrane current-induced thermal damages in the delayed rectifier K^+ channels. A double Vaseline-gap voltage clamp was used to deliver shock pulses and to monitor the channel currents. Three pairs of 4-ms shock pulses were used to mimic the electric shock by a power-line frequency electric field. Each pair consists of two pulses with the same magnitude, starting from 350 to 500 mV, but with opposite polarities. The shock pulse-generated transmembrane ion flux and the responding electric energy, the Joule heating, consumed in the cell membrane, as well as the effects on the K^+ channel currents, were obtained. Results showed that huge transmembrane currents are not necessary to cause damages in the K^+ channel proteins. In contrast, reductions in the K^+ channel currents are directly related to the field-induced supramembrane potential differences. By a comparison with the shock field-induced Joule heating effects on cell membranes, the field-induced supramembrane potential difference plays a dominant role in damaging the K^+ channels, resulting in electroconformational changes in the membrane proteins. In contrast, the shock field-induced huge transmembrane currents, therefore the thermal effects, play a secondary, trivial role.

INTRODUCTION

An electric field, as a tool, has been widely used in today's medical diagnosis and treatments. For example, defibrillation and pacemakers are common techniques used to reinstall the normal cardiac cell functions (Lau and Camm, 1991; Raymond et al., 1991). Membrane electroporation has been widely used to increase the efficiency of gene transfection and cell fusion (Winegar et al., 1989; Zimmermann et al., 1980; Chang et al., 1991). Electroporation was also suggested for use on skin stratum corneum for transdermal drug delivery (Okino and Mohri, 1987; Mir et al., 1991; Bommannan et al., 1993; Prausnitz et al., 1993).

Alternatively, the mechanisms involved in electrical trauma remain unclear. Better understanding of the mechanisms in electrical injury will significantly improve our diagnosis and treatment of electrically injured patients.

The electric resistance of the cell's phospholipid bilayer is six to eight orders of magnitude higher than those of cytoplasmic and extracellular electrolytes. When living cells are exposed to an external electric field, most of the field-induced voltage-drops fall on the cell membranes. In addition, since the cell dimension is a few orders of magnitude larger than the thickness of the cell membrane, the induced equivalent field strength inside the cell membrane is hundreds and thousands times higher than the apparent strength of the applied electric field (Cole, 1972). Under such a high field strength, the field-induced membrane potential difference is much higher than those in physiological condition. These supraphysiological potential differences or supramembrane potential differences may cause damage in membrane phospholipid bilayer and membrane proteins.

One of the possible mechanisms involved in electrical injury is Joule heating. The direct effects of Joule heating in damaging cells and tissues has long been recognized as denaturation of the cell membrane and membrane proteins (Cravalho et al., 1992; Tropea and Lee, 1992). Toner et al. investigated thermal-mediated injury in isolated skeletal muscle fibers by study of quantitative microscopy of membrane permeability changes at supraphysiological temperatures in isolated muscle cells and fibroblasts (Bischof et al., 1995). Joule heating-induced membrane damage is known to be proportional to electric energy consumed in the cell membrane, which is directly related to the field-induced transmembrane currents (Rouge and Dimick, 1978; Lee et al., 1988).

In addition, membrane electroporation was also considered as one of the mechanisms of electrical trauma (Lee and Kolodney, 1987; Jones et al., 1987; O'Neill and Tung, 1991; Chen et al., 1992). In contrast to Joule heating caused by a huge transmembrane current, field-induced supramembrane potential difference plays a significant role in membrane electroporation (Kinosita and Tsong, 1977). Membrane electroporation has been postulated mainly as the supramembrane potential difference-induced electroconformational damages in the phospholipid bilayer (Tsong, 1991). Resealing of the membrane electropermeabilization under the control of cytoskeletal proteins is also considered as an alteration of the membrane organization or the consequence of the associated cytoplasmic content (Teissie and Rols, 1994).

Received for publication 17 July 1997 and in final form 26 March 1998.
Address reprint requests to Dr. Wei Chen, Department of Dermatology, The University of Illinois at Chicago, 808 South Wood St., Chicago, IL 60612. Tel.: 312-413-2448; Fax: 312-996-1188; E-mail: weichen@uic.edu.

0006-3495/98/07/196/11 $2.00

An intensive electric field also affects the membrane proteins, especially the voltage-sensitive proteins. In fact, structural features of many membrane proteins suggest a large susceptibility to electric fields. Functions of these electric field-sensitive membrane proteins can therefore be affected by the transmembrane potential (Eisenberg et al., 1987; Tsong and Astumian, 1987). A high-intensity electric field may further cause electroconformational damages in these membrane proteins. Tsong and his colleagues (Teissie and Tsong, 1980; Tsong and Astumian, 1986) showed that an intensive shock field could induce leakage currents through membrane proteins, the Na^+/K^+ ATPase of erythrocyte cell membranes. They attributed the field-induced leakage as the membrane proteins' electroconformational damages. Recently, electric field-induced damages in membrane proteins have been considered as a mechanism involved in electrical injury (Chen and Lee, 1994b, Abramov et al., 1997). We have found that a brief high-intensity electric shock can cause not only membrane electroporation, but also reductions in the K^+ channel conductance and ionic selectivity.

A detailed study to identify whether the membrane protein functional reductions result from the protein electroconformational damages or from the field-induced Joule heating has not been conducted yet. The former caused by a supramembrane potential may involve movements of the charge particles, or reorientations of the equivalent dipole moments in the channel proteins, while the latter caused by a huge transmembrane current may involve a local temperature increase leading to an electrical burn in the narrowest pores of the channel proteins.

In this paper we try to understand which among the supramembrane potential difference-induced electroconformational changes and the huge transmembrane current-mediated thermal effects is the dominant mechanism involved in membrane protein damages. We distinguished these two mechanisms by comparing the K^+ channel functional reductions with the huge transmembrane current-induced Joule heating effects.

To perform these experiments, an improved double Vaseline-gap voltage clamp technique was used to mimic electric shock by direct delivery of shock pulses to the cell membrane. The evoked transmembrane currents were simultaneously monitored during the shock so that the electric energy consumed in the membrane could be studied. The K^+ channel functions were monitored before and after the electric shocks. The shock-induced damages in the channel proteins were obtained and compared with the Joule heating effects. The results showed that shock field-induced reductions in the K^+ channel currents depend mainly on the field-induced supramembrane potential difference, but not necessarily on the supratransmembrane currents. The results clearly indicate that within a certain intensity range, the field-induced electroconformational changes play a dominant role in the mechanism of electrical trauma.

MATERIAL AND METHODS

Skeletal muscle fiber preparation

The protocol for single fiber preparation was followed (Hille and Campbell, 1976; Kovacs et al., 1983; Irving et al., 1987; Hui and Chen, 1997) with some adjustments (Chen and Lee, 1994a–c). Briefly, skeletal twitch muscles (semitendinosus) were separated from either English frogs, *Rana temporaria*, or American frogs, *Rana Pipe*. Single fibers were hand-dissected and mounted in a custom-made chamber with two clips at the ends for fiber attachment. The fibers were electrically isolated in three pools by two Vaseline-gap partitions. The width of the two partitions and the width of the central pool are 100 μm and 300 μm, respectively. The fibers were stretched up to the length of a sarcomere of 3 μm to avoid fiber contraction during electrical stimulations.

The fiber segments in two endpools were treated with a solution with 0.2% saponin for 2 min and then washed out with the internal solution, where the fiber segments were permeabilized electrically and ionically. The three pools were then connected to the voltage clamp by six agar bridges and three Ag/AgCl pallets. Resistance of these bridges and pallets was <1 kΩ. Both stimulation pulses and shock pulses were delivered through a computer-controlled voltage clamp (Dagon 8800 whole clamp). Data were sampled by an Axon data acquisition board (AC 1200) and stored in disks for further analysis.

Composition of solution

The composition of each solution was as follows (in mM): Relaxing solution: 120 potassium glutamate; 1 $MgSO_4$; 0.1 EGTA; 5 PIPES. External solution: 120 NaCl; 2.5 KCl; 2.15 Na_2HPO_4; 0.85 NaH_2PO_4; 1.8 $CaCl_2$. One μM TTX was added to block the sodium channels. Internal solution: 45.5 potassium glutamate; 20 Tris-Creatine phosphate; 20 EGTA; 6.8 $MgSO_4$; 5 PIPES; 5 glucose; 5.5 Na_2ATP.

Electric shock and channel function recording

We have suggested an improved configuration of the double Vaseline-gap voltage clamp to study the electrical injured cell membranes in skeletal muscle fibers (Chen and Lee, 1994a, b). Briefly, the two endpools were connected and a positive feedback circuit was used to compensate voltage drops on the series resistance underneath the two Vaseline partitions. The advantages of the improved configuration include a more uniform membrane potential-distribution in the central pool and an elimination of the transient overshock at the rising phase of the shock pulse. The protocol of the experiments was designed to investigate the shock-induced membrane electroporation and damages in the voltage-gated K^+ channels.

The membrane holding potential was -90 mV. Two pulse groups were used in this study. Stimulation pulses, a sequence of 30-ms-duration pulses ranging from 30 to 120 mV, held the membrane potential from -60 to 30 mV. Shock pulses within a supraphysiological membrane potential range from -200 mV to -600 mV were delivered by the voltage clamp to the cell membranes. The duration of all shock pulses was 4 ms to mimic the electric shock by a field with power-line frequency. Before the application of a shock pulse, the stimulation sequence was applied to the cell membrane and the evoked K^+ channel currents were recorded.

Then a supramembrane potential pulse was delivered to the membrane and the evoked transmembrane currents were simultaneously monitored during the shock. There are two advantages of simultaneously monitoring the shock-induced transmembrane currents. First, we were able to quickly identify an occurrence of electroporation current. Second, the simultaneous measurements of transmembrane current and membrane potential difference allowed us to study the electric energy consumed in the cell membrane, which is proportional to the transmembrane currents. Right after the pulsed shock the same stimulation sequence was delivered again to the membrane to distinguish the shock-induced effects on the K^+ channel

currents. A P/N method was used to identify channel currents and electroporation currents. Briefly, four substimulation pre-pulses preceding each stimulation pulse were employed to measure the linear transmembrane currents. The magnitude of the substimulation pre-pulses was one-fourth of that of the immediately following stimulation pulse. Since the magnitude of the pre-pulses is far below the K^+ channel open threshold, the elicited currents were only the linear leakage currents and capacitance currents, which were proportional to the membrane potential differences. These linear currents were then scaled up and subtracted from the stimulation pulse-evoked total transmembrane current. The remaining currents were the voltage-dependent K^+ channel currents. With the same method, by using a group of pre-shock subpulses, the shock pulse-induced electroporation current can be resolved. The only difference is that the number of subshock pre-pulses was higher than four, so that the magnitude of each pre-pulse is far below the electroporation threshold.

RESULTS

Shock pulse-induced reductions in the K^+ channel conductance

We started from a measurement of the delayed rectifier K^+ channel currents in cell membranes. A stimulation pulse sequence consisting of 15 consecutive pulses held the cell membrane potential from −60 mV to 10 mV with 5-mV increments. The evoked transmembrane currents were recorded (not shown). By using the P/N method, the nonlinear voltage-dependent K^+ channel currents were resolved and are shown in the upper panel of Fig. 1. The maximum

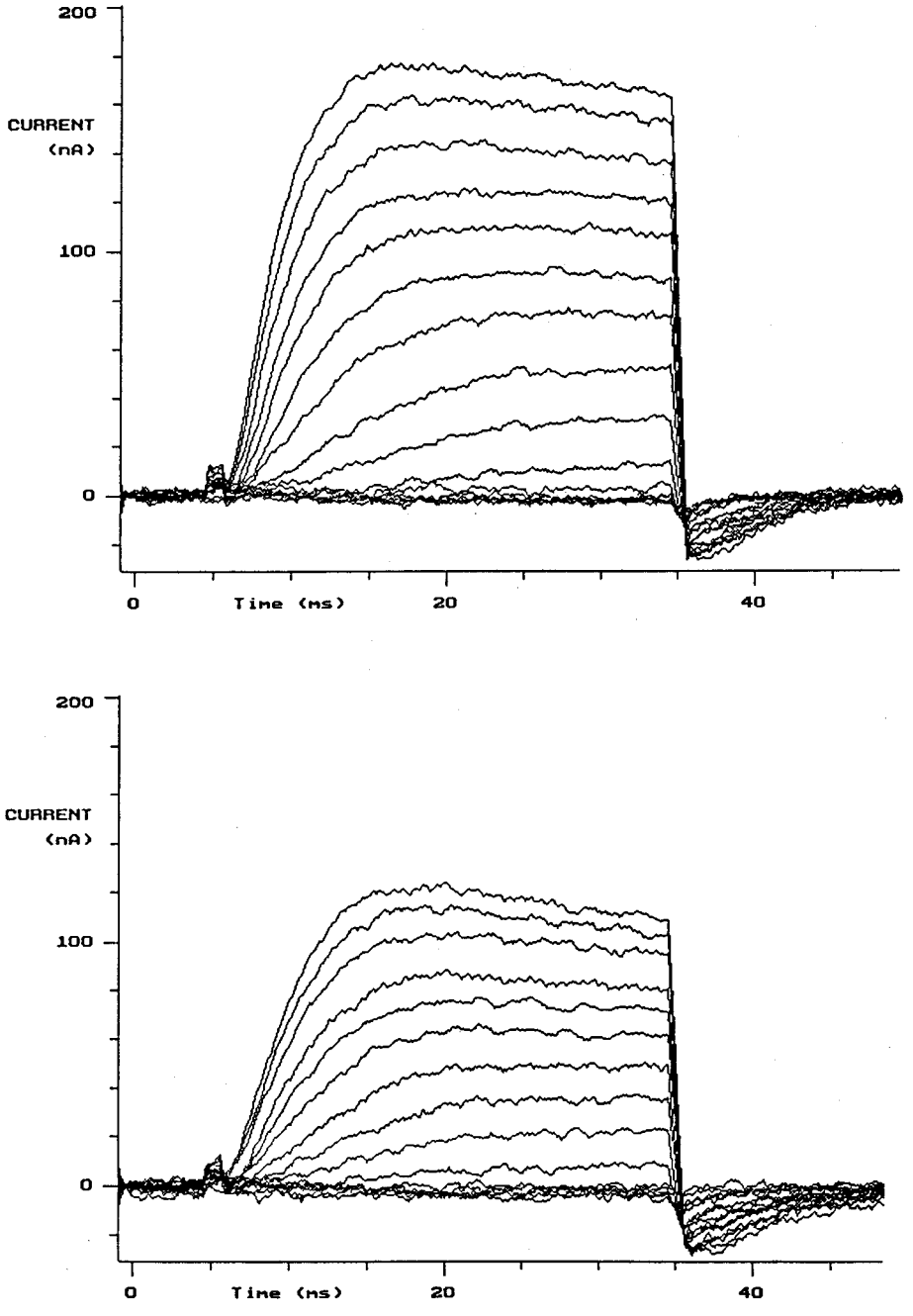

FIGURE 1 The pre- and post-shocked K^+ channel currents responding to a stimulation sequence consisting of 15 consecutive stimulation pulses. The linear leakage currents crossing the cell membrane or through the pathway underneath the Vaseline seals were recorded by using four substimulation pre-pulses. These linear leakage currents were then scaled up and subtracted from the stimulation pulse-evoked total transmembrane current. The remaining voltage-dependent K^+ channel currents are shown in the figure. The top panel shows the pre-shocked K^+ channel currents. After being shocked by a 4-ms, −400 mV pulse, the channel currents were immediately recorded and are shown in the bottom panel.

channel current is ~180 nA, a response to a stimulation pulse holding the membrane potential difference of 10 mV.

Then, a 4-ms shock pulse with a supramembrane potential difference of −400 mV was delivered by the voltage clamp to electrically shock the cell membrane. The evoked total transmembrane current was simultaneously recorded and is shown in the top panel of Fig. 2. The first transient peak current with an exponential decay represents the membrane capacitance currents. The following monotonously increasing current is the shock pulse-induced electroporation current. This electroporation current is defined as a shock field-induced nonlinear leakage current. The linear

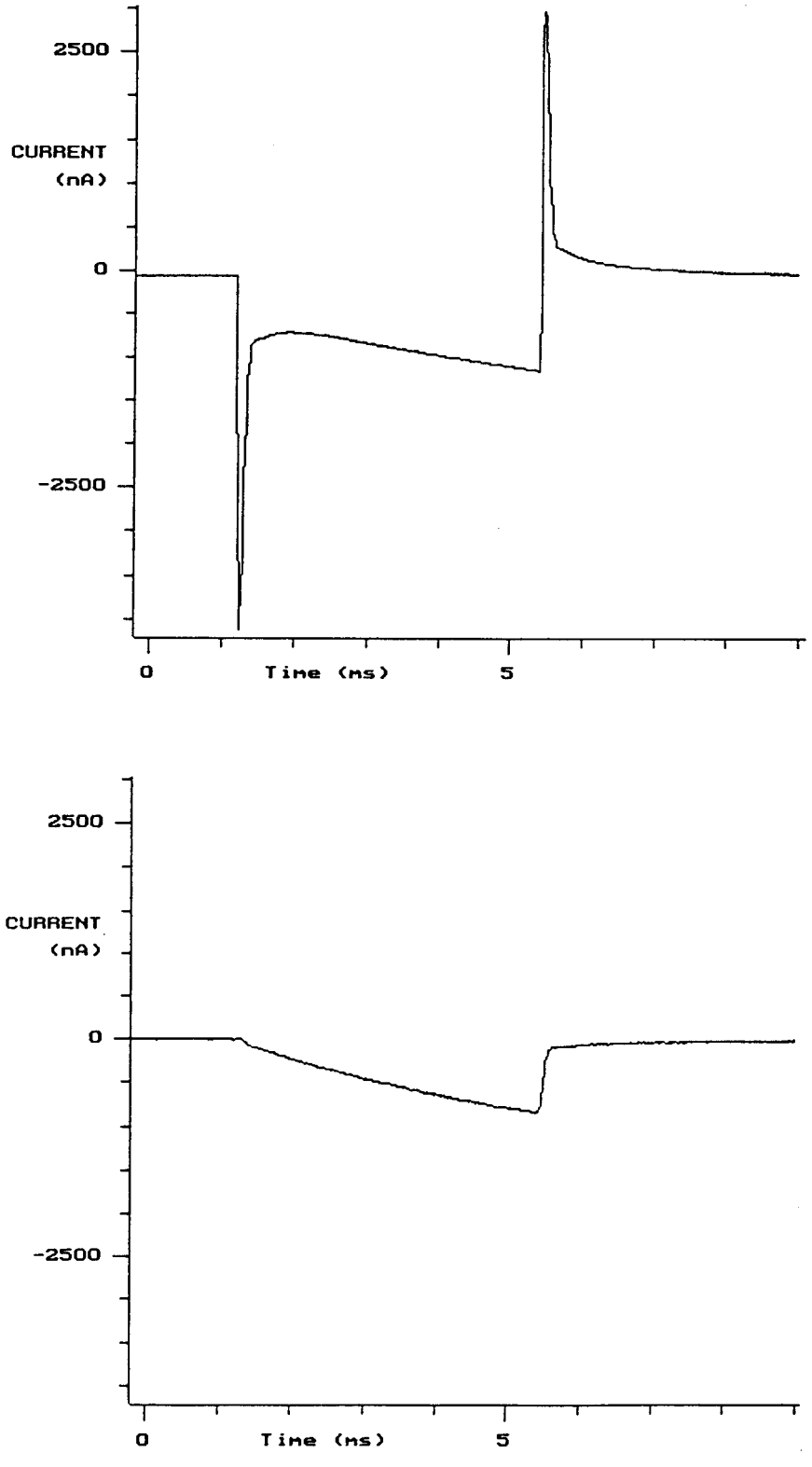

FIGURE 2 Transmembrane currents recorded during a 4-ms, −400 mV pulsed shock. *Top:* the total transmembrane currents. The transient peak current with an exponential decay represents the membrane capacitance current. The following monotonously increasing current is the shock pulse-induced electroporation current. By subtracting linear leakage and capacitance currents recorded from subshock pre-pulses, the electroporation current was explicitly obtained and is shown in the bottom panel. For this fiber, a single 4-ms, −400 mV shock pulse generated over 800 nA electroporation current.

transmembrane currents were recorded by applying five subshock pre-pulses in a magnitude of −80 mV, which was far below the membrane electroporation threshold of −300 mV (Chen and Lee, 1994a). By subtracting these linear leakage and capacitance currents from the total shock current, the electroporation current could be explicitly obtained and is shown in the bottom panel of Fig. 2. For this fiber, a single 4-ms, −400 mV shock pulse generated up to over 800 nA electroporation currents.

After the electric shock, the same stimulation pulse sequence was reapplied to the cell membrane. With the same method the K^+ channel currents were resolved and are shown in the bottom panel of Fig. 1. By comparing the pre- and post-shock channel currents, one can easily notice that the magnitudes of the K^+ channel currents were significantly reduced after a brief electric shock. The maximum value of the K^+ channel current for this fiber dropped from ~180 nA to ~125 nA, a >30% reduction from the original value.

Damaging effects of the supramembrane potential difference on cell membrane are directional

From the difference of the pre- and post-shock channel currents responding to the same stimulation pulses, we demonstrated that after the cell membrane was shocked by a single 4-ms, −400 mV pulse, the K^+ channel conductance reduced over 30%. The results also showed that the brief pulsed shock could damage the cell membranes generating a huge transmembrane current. However, the uncertainty is how this huge transmembrane current raised membrane temperature, thereby damaging the membrane proteins.

During the experiments, we had tried to use a microthermistor to monitor the possible temperature changes caused by high-voltage shock pulses. Because of low temperature-resolution and slow time-constant, it is impossible to use a thermistor to monitor local and transient temperature changes on the cell membranes. To investigate the field-induced thermal effects on cell membrane we need to study the electrical Joule heating by identifying the electric energy consumed in the cell membranes, by using our voltage clamp techniques to simultaneously measure membrane potential differences and transmembrane currents.

A new fiber was prepared by using the same method described above. The stimulation sequence was applied to the cell membrane. By subtracting the linear capacitance and leakage currents, the K^+ channel currents were resolved with a maximum value of 168 nA (data not shown).

The fiber was then shocked by a series of pulse pairs, each pair consisting of two pulses with the same magnitude but different polarities. The time interval between the two pulses in each pair was 5 min, and the pulse pairs were separated by 10 min to allow full relaxation of the fiber. The positive shock pulse in each pair was always applied to the fiber before the negative pulse, since a positive shock pulse causes much less damage in channel proteins than a negative pulse of the same magnitude (see the results). The corresponding transmembrane currents during the shock pulses were simultaneously recorded. After each shock, the same stimulation sequence was applied to the cell membrane to monitor the shock pulse-induced reductions in the channel activity.

The left panel of Fig. 3 shows the total transmembrane current responding to a 4-ms, +350 mV shock pulse, while a −350 mV shock pulse-generated total transmembrane current is presented in the left panel of Fig. 4. Although the membrane potential differences were the same held by the voltage clamp, the responding currents are significantly different. In Fig. 3, the transient capacitance current is followed by a huge K^+ channel current. At end of the shock pulse, the transmembrane current was slightly increased, which may be due to the membrane electroporation. This is because that −350 mV is higher than the membrane electroporation threshold (Chen and Lee, 1994a; Tovar and Tung, 1992). The peak value of the positive shock pulse-evoked total transmembrane current (except the transient capacitance current) is ~2200 nA (*left panel* of Fig. 3). Because the fiber was hyperpolarized, no channel currents are observed in Fig. 4. The slightly increased current at the end of the shock pulse may also be the membrane electroporation current. The maximal value is <200 nA (*left panel* of Fig. 4). The positive shock pulse depolarized the cell membrane and opened the K^+ channel, resulting in a total transmembrane current much larger than those evoked by the negative shock pulse.

The right panels of Figs. 3 and 4 represent the stimulation sequence-evoked K^+ channel currents recorded immediately after the positive and negative shocks, respectively. The maximum value of the K^+ channel currents is 165 nA in Fig. 3 and 140 nA in Fig. 4. Compared to the maximum K^+ channel currents (168 nA) obtained before the shocks, the +350 mV shock pulse had little, if any, effect on the channel currents. However, the single 4-ms, −350 mV shock pulse reduced the channel currents ~17%. It should be pointed out that the positive shock pulse caused a transmembrane current 10 times larger than the negative shock pulse, but had almost no effect on the K^+ channel currents.

A comparison of the field-induced ion flux across the cell membrane

According to Joule's law, when the environment remains the same, the field-induced evolution rate of heat on the cell membrane should be equal to the shock pulse-induced electric energy consumed on the cell membrane. We can estimate the consumed energy by integrating the transmembrane resistive currents with time during the 4-ms shock pulse and then multiplied by the applied membrane potential difference. Since most of the external field-induced potential difference is across the cell membrane, the estimated electric energy should be mainly consumed in the cell membranes, which represents the process of transmembrane heating.

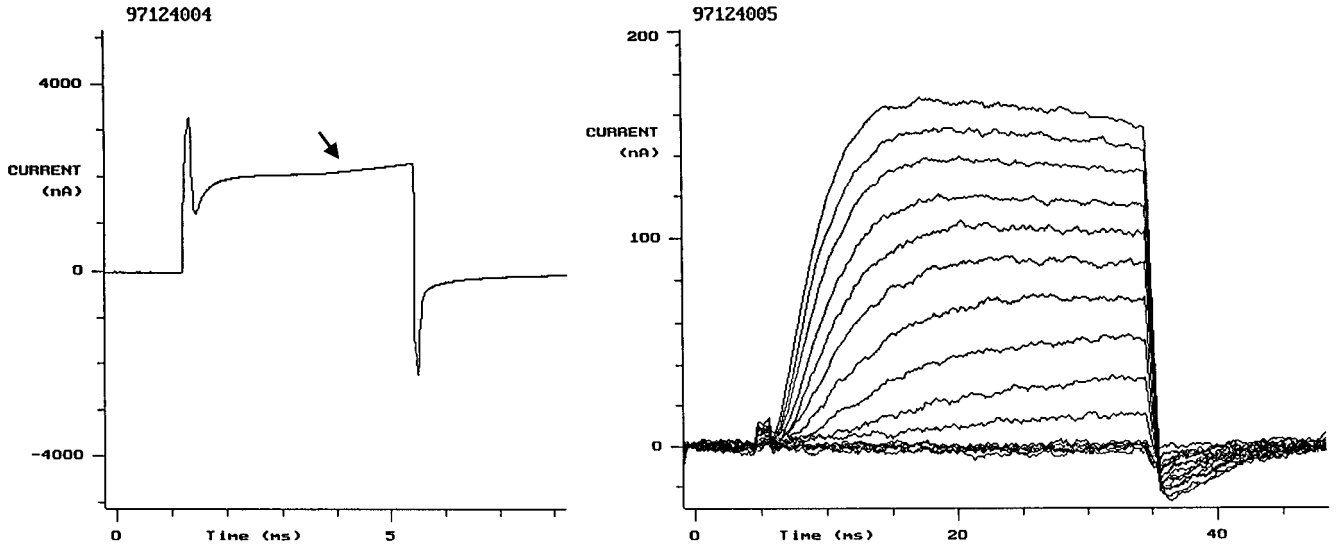

FIGURE 3 The total transmembrane currents induced by a supramembrane potential shock and the post-shocked K^+ channel currents. In the left panel are shown the total transmembrane currents responding to a 4-ms, +350 mV shock pulse. The peak value of the resistive current in the total transmembrane currents is 2200 nA. From about the last millisecond (marked as an arrow) of the shock pulse, the transmembrane current is slightly increased, which is due to the membrane electroporation. It clearly shows that the majority of the transmembrane resistive current is the K^+ channel current. The right panel represents the stimulation sequence-evoked K^+ channel currents recorded immediately after the shock. The maximum value of the K^+ channel currents is 165 nA.

Because of the difficulties in identifying the pathway of the shock pulse-induced transmembrane currents, we first simply considered the Joule heating as a bulk Joule heating in the cell membrane. The local Joule heating effects on specific membrane proteins, the K^+ channels, will be further discussed later.

Since the capacitance currents are the intramembrane displacement currents, they should be subtracted from the total responding currents when estimating the Joule heating effects. To subtract the transient capacitance current, the monotonously decreasing data points after the transient peak were fitted by an exponential decay curve. The resistive current crossing the cell membrane can be obtained by subtracting the transient capacitance current with the fitted exponential decay curve. The resultant resistive current contributed to the real electric energy consumed on the cell membrane.

By integrating the transmembrane resistive current obtained from the left panel of Fig. 3, the electric charge passing through the cell membrane is 8.2 nC in response to

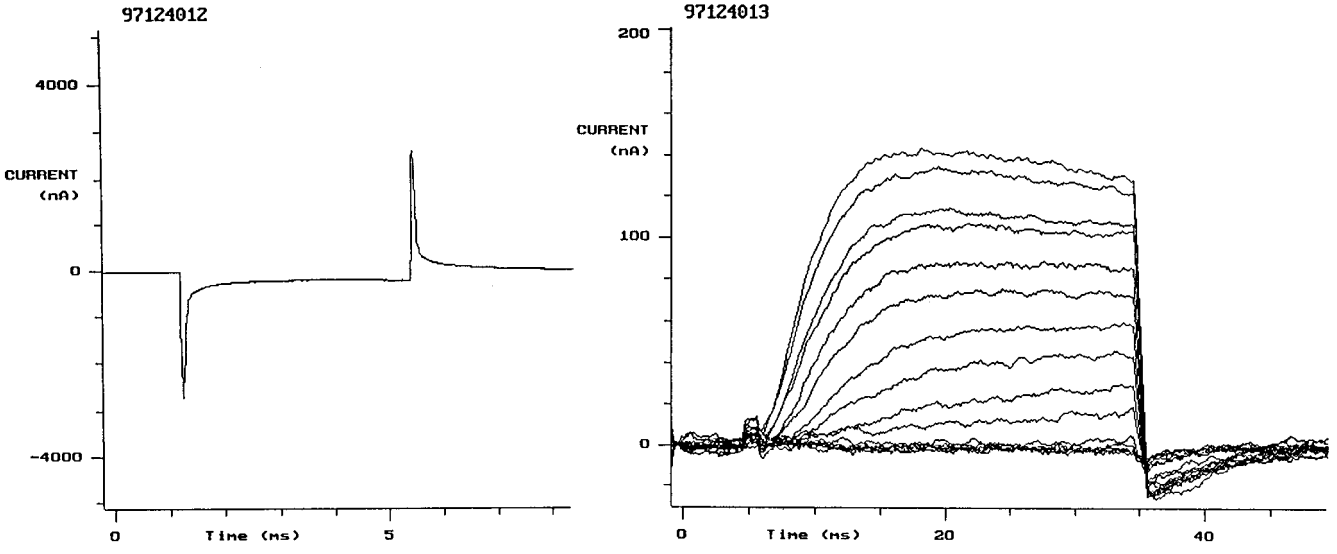

FIGURE 4 The total transmembrane currents evoked by a supramembrane potential, −350 mV shock and the post-shocked K^+ channel currents. Because of fiber being hyperpolarized, no channel currents were observed. Because of proximity to the electroporation threshold, little electroporation current was generated at the end of the shock pulse. The maximum values of the resistive current and the K^+ channel currents are $<$200 nA and $\sim$165 nA, respectively.

a +350 mV pulse. Only 0.9 nC charges passed through the cell membrane during the −350 mV shock pulse, obtained from the left panel of Fig. 4. Although generating 8.2-nC charges crossing the cell membranes, the +350 mV shock pulse caused little (3 of 168 nA) decrease in the K^+ channel currents. In contrast, the −350 mV shock pulse, generating only 0.9-nC transmembrane charges, almost one-tenth of those induced by the positive-shock pulse, significantly decreased the K^+ channel currents, from 168 nA to 140 nA. This comparison clearly shows that electric field-induced reduction in the K^+ channel currents is not directly related to the amount of transmembrane currents.

After the fiber was relaxed at the membrane holding potential of −90 mV for 10 min, a pair of shock pulses of magnitude 500 mV but opposite polarities was applied to the cell membrane. The positive pulse-evoked total transmembrane current was recorded, as shown in the left panel of Fig. 5. Because of the shock pulse far beyond the electroporation threshold, the electroporation current dominates the total transmembrane current with a maximum value over the limitation of our equipment, 5000 nA. After the pulsed shock, the K^+ channel currents were recorded and are shown in the right panel of Fig. 5. Interestingly, the maximum peak value of the K^+ channel currents shows little reduction, from 168 nA to 158 nA. Five minutes later, the same magnitude but negative shock pulse was applied to the cell membrane, and the evoked transmembrane current was recorded as shown in the left panel of Fig. 6. A huge electroporation current occurred with a maximum value of the resistive current of 3800 nA, leading to a significant reduction of the post-shock K^+ channel currents from 168 nA to 105 nA, as shown in the right panel of Fig. 6.

With the same method, transient capacitance current was obtained by an exponential decay curve fitting, and subtracted from the total transmembrane currents to resolve the resistive current. The integrations of the resistive currents with time showed at least 17.4 nC of transmembrane charges during the +500 mV shock pulse, while only 10.4 nC charges were driven across the cell membrane by the −500 mV pulse.

The −500 mV pulse, which generated 10.4 nC charges crossing the cell membrane, significantly reduced the K^+ channel currents (from 168 to 105 nA), while the +500 mV shock pulse, which drove a much larger amount of transmembrane charges (17.4 nC), had little effect on the K^+ channel currents (from 168 nA to 158 nA). Table 1 summarizes the results from Fig. 3 to Fig. 6.

A comparison of the field-induced Joule heating on the cell membrane

When we cross-reference the shock potentials and the evoked transmembrane currents with the shock-induced channel current reduction in response to −350 mV and +500 mV shock pulses (second and third columns of Table 1), the results are even more conclusive. The −350 mV shock pulse generating <200 nA of maximum leakage currents resulted in a total transmembrane charge of only 0.9 nC. However, the K^+ channel currents showed a significant reduction, from 168 nA to 140 nA, ~17%. In contrast, the +500 mV pulse generating a leakage current far beyond 5000 nA resulted in 17.4 nC ions crossing the cell membranes. Interestingly, this +500 mV shock had little effect on the K^+ channel currents, from 168 nA to 158 nA, only 6% reduction. The +500 mV shock pulse generated over 18 times higher transmembrane charges than the −350 mV shock pulse, but caused only one-third of the reduction in the K^+ channel currents.

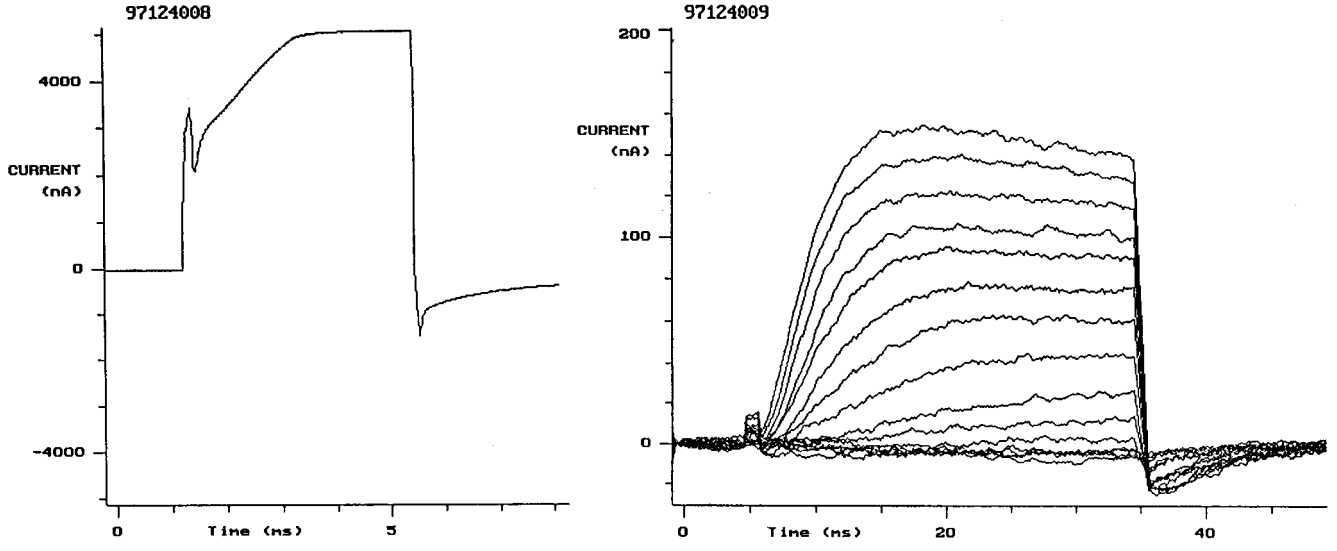

FIGURE 5 The total transmembrane current induced by a +500 mV shock pulse and the post-shocked K^+ channel currents. Because they are far beyond the potential threshold of membrane electroporation, the possible electroporation current is far over the limitation of our equipment, 5000 nA. Interestingly, the peak value of the K^+ channel current has a little reduction, from 168 nA to 158 nA.

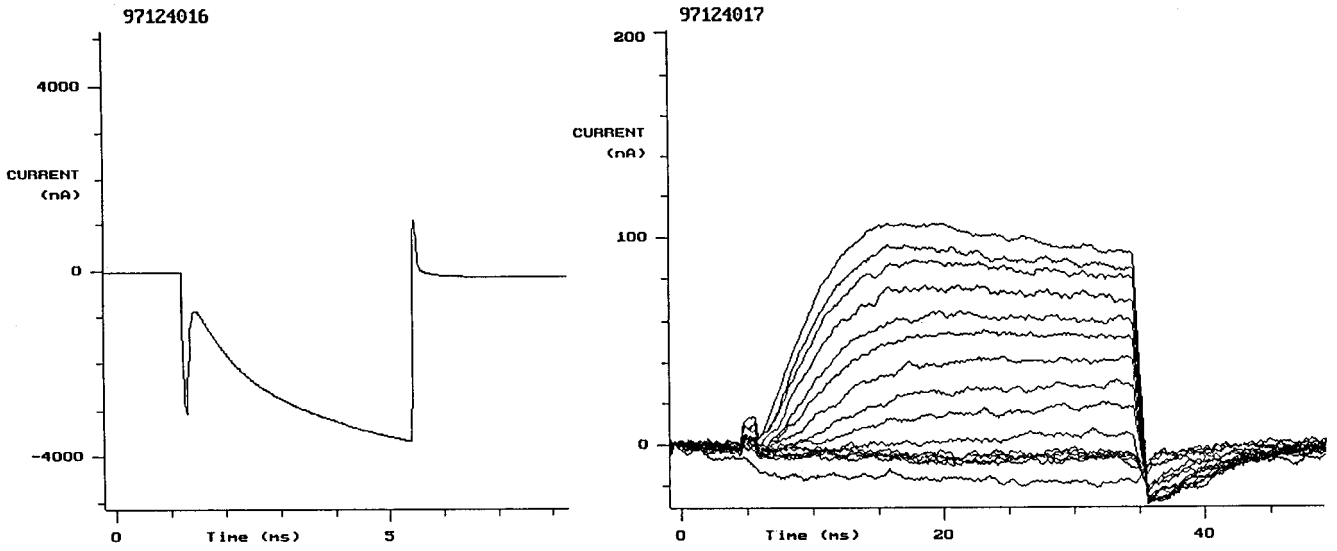

FIGURE 6 A −500 mV shock pulse-generated total transmembrane current and K^+ channel currents recorded thereafter. The left panel shows a huge value of electroporation current with a maximum resistive current of 3800 nA. Consequently, the magnitude of the post-shocked K^+ channel currents were significantly reduced to 105 nA.

Furthermore, considering the difference of the membrane potential, the +500 mV shock pulse generated 29 times more thermal effects, the Joule heating on the cell membrane, but caused only one-third reduction in the K^+ channel currents when compared with a −350 mV shock. These results imply that the intensive electric field-induced damages in the K^+ channel proteins should not be attributed to the field-induced supramembrane currents, therefore the current-mediated thermal effects on the cell membranes. In other words, the shock field-induced damage is mainly due to the supramembrane potential difference-induced electroconformational changes in the protein structures, which are primarily dependent on the membrane potential.

Thirteen fibers have been investigated to distinguish the effects of the supramembrane potential and huge transmembrane current on the K^+ channel currents. The same experimental protocol with three pairs of shock pulses (350, 400, and 500 mV) and opposite polarities in each pulse pair was used. To increase the capability of current injection, a high compliance-voltage mode of the voltage clamp was used. The maximum injecting current is 13,000 nA, far beyond a 500 mV pulse-evoked total transmembrane current. The K^+ channel currents recorded after each shock pulse are plotted in Fig. 7. The dark and open columns represent the channel currents recorded after the fibers were shocked by positive and negative pulses, respectively. It clearly shows that negative shock pulses cause much larger reductions in channel current than the positive shock pulses. Fig. 8 shows the shock pulse-generated transmembrane charges, obtained by integration of the evoked resistive transmembrane current. The positive shock pulse drove much larger amounts of charges across the cell membranes, but had little effect on the K^+ channel currents.

Fig. 9 shows the comparison of the shock pulse-induced Joule heating on the cell membranes and the reduction percentage in the K^+ channel currents in response to shock pulses of −350 mV and +500 mV, respectively. Single

TABLE 1 Transmembrane charges and channel functional reduction responding to different shock pulses

Shock Pulses	+350 mV	−350 mV	+500 mV	−500 mV
Transmembrane charges (nC)	8.2	0.9	17.4	10.4
Channel functional reduction (%)	1.8	17	6	37.5

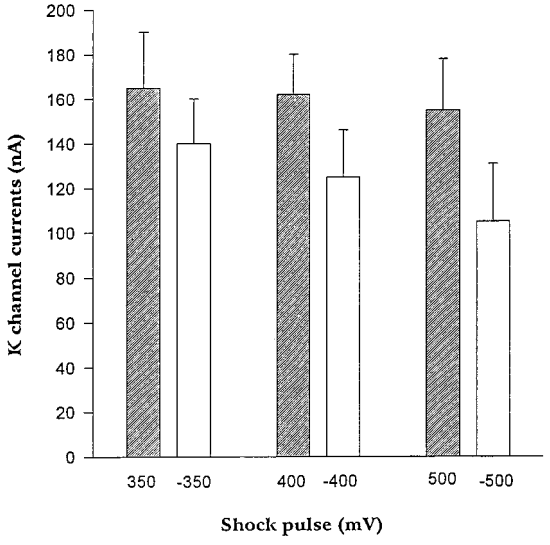

FIGURE 7 The shock pulse-induced reduction in the K^+ channel currents. The dark columns represent the post-shock K^+ channel currents recorded after the positive shock pulses, and the open columns represent the post-shock channel currents recorded after the negative shock pulses. The bars represent standard deviations.

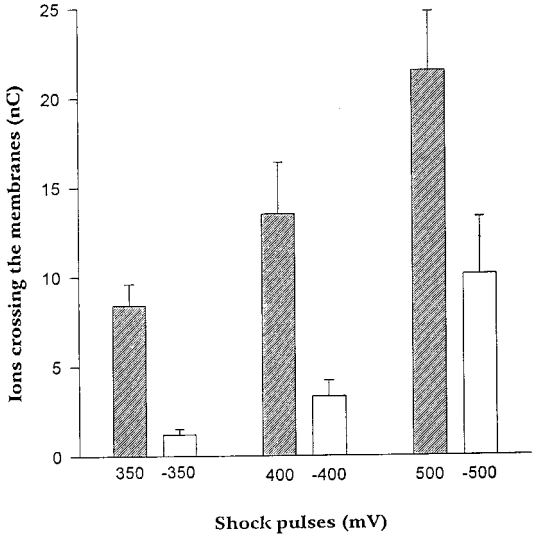

FIGURE 8 Ion flux driven by different shock pulses. The dark columns represent the integrated transmembrane ion flux obtained during the positive shock pulses and the open columns represent the ion flux during the negative shock pulses. Because of opening channels, positive shock pulses generated much larger transmembrane ion flux than negative shock pulses. The bars represent standard deviations.

4-ms, −350 mV shock pulses driving 1.2 nC charges crossing the cell membrane generated 0.42 nJ heat, but caused ~17% reduction in the K^+ channel currents. In contrast, single 4-ms, +500 mV shock pulses eliciting 21 nC transmembrane charges generated Joule heating of 10.7 nJ. The K^+ channel currents were only reduced by ~8%. When compared with a −350 mV shock, a +500 mV pulse drove ~18 times more charges across the cell membrane, thereby generating 25 times more Joule heating on the membrane, but it only caused less than one-half of the reduction in the K^+ channel current.

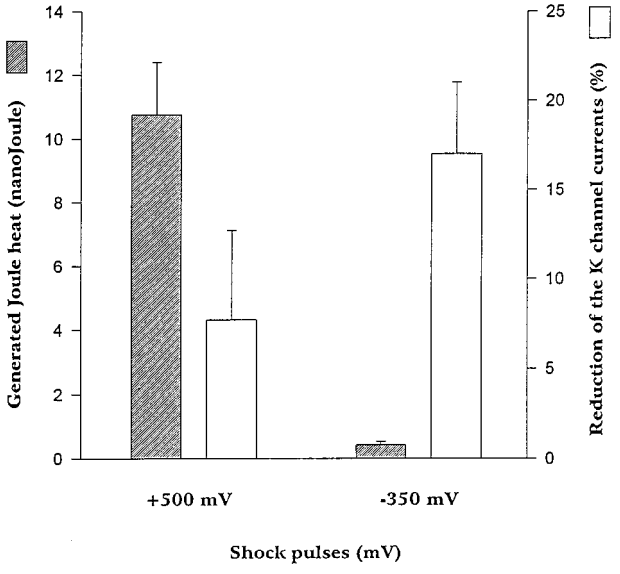

FIGURE 9 A comparison of the shock pulse-induced Joule heating effects with the induced percentage reductions in the K^+ channel currents when shocked by 4-ms pulses of −350 mV and +500 mV, respectively. The dark columns represent the shock pulse-induced Joule heating effects in a scale of nanojoules, shown as the left ordinate. The open columns represent the percentage reductions in the K^+ channel currents shown as the right ordinate. The bars represent standard deviations.

DISCUSSION

Shock-induced channel function reduction is not directly related to the huge transmembrane currents, therefore it should not be attributed to the cell membrane Joule heating effects

The main point of this study is to compare supramembrane potential difference-induced effects on the K^+ channels and supratransmembrane current-mediated Joule heating on the cell membranes. Pulse pairs with the same magnitude but opposite polarities were employed to differentiate these two effects. Positive shock pulses that depolarized the membrane potential opened the K^+ channels, generating huge channel currents as well as some electroporation currents. However, there was no significant reduction in the K^+ channel currents, at least not for a shock pulse up to +500 mV. In contrast, negative shock pulses that hyperpolarized cell membranes, inducing many fewer transmembrane currents, caused a significant decrease in the K^+ channel currents.

These results clearly indicate that electric shock pulse-induced damage is not necessarily due to the field-induced supratransmembrane current which, when multiplied by the membrane potential difference, is equal to the electric field-induced Joule heating on the cell membranes. In contrast, the protein channels' damages directly depend upon the polarity and magnitude of the shock pulses.

It is necessary to point out that cell membrane is inhomogeneous, and the electric energy consumed in the cell membrane and therefore the Joule heating are not uniformly distributed in the cell membranes. In fact, results from others (Mehrle et al., 1985; Sower and Lieber, 1986; Kinosita et al., 1992) and our laboratory (Chen and Lee, 1994c) suggested that a cell membrane asymmetry is present, which may be mainly related to membrane proteins' insertion. In addition, a very localized heating effect may also take place when a heavy current occurs along the well-defined narrow pathways, giving a local temperature increase. Using the macromeasured membrane potential difference and transmembrane currents to obtain the Joule heating on the cell membranes is only a global Joule heating in whole cell membrane.

Shock pulse-induced reduction in K^+ channel functions is not directly related to local Joule heating on the channel proteins

After the exclusion of the possibility of the global Joule heating as the cause for the reductions in the K^+ channel activities, we now focus on the specific membrane protein

Joule heating; in this case, the K^+ channels. First, we need to fully understand what our integrated ion flux means. For the currents responding to the positive shock pulses, after subtracting the curve-fitted capacitive currents, the remaining resistive currents include linear leakage current, channel current, and electroporation current. For the currents responding to the negative shock pulse, the remaining currents include only the linear leakage current and the electroporation currents because the negative pulse hyperpolarized the cell membrane and closed most of the K^+ channels. The ideal way to discuss local Joule heating on the K^+ channel proteins is to identify the shock-induced channel currents by subtracting the linear leakage current and the membrane electroporation current from the total transmembrane currents. However, it is technically difficult to realize, since both channel current and membrane electroporation current are nonlinear currents. It is impossible to use the P/N method to distinguish two nonlinear components.

Even though we cannot quantitatively identify the pure current passing through the K^+ channel during the shock pulses, it does not affect our qualitative analysis. As an example, let's go back to the comparison of the channel function reduction caused by either a +350 mV or a −350 mV shock pulse. From Table 1 we showed that a +350 mV shock pulse generated >9 times more Joule heating in the cell membrane than a −350 mV shock pulse (current ratio = 8.2:0.9 with the same magnitude of the membrane potential difference), while only causing a 1:9 (ratio = 1.8:17) reduction of the channel currents. Since the magnitude of the shock pulses are the same, the induced linear leakage currents should be the same, which is proportional to the membrane potential difference. We now only have to distinguish the channel currents from the membrane electroporation currents (through the phospholipid bilayer).

Voltage-dependent differences and current kinetic characteristics of each current component can be used to differentiate the channel currents from the membrane electroporation currents. Kinetic studies of the delayed rectifier K^+ channels showed that the channel currents, after a short delay, have a long, flat plateau (Hille, 1992). Our previous studies and this study (Fig. 2) showed that electroporation current monotonously increases during the shock pulse (Chen and Lee, 1994a). From the left panel of Fig. 3, it is clearly shown that the majority of the resistive current responding to a +350 mV pulse was carried by the K^+ channels, and the membrane electroporation current was very small, seen from the relative flat plateau of the resistive current. We have estimated that >95% of the resistive currents are attributed to the channel current by fitting the early part of the plateau to a horizontal straight line in order to separate the channel currents and the electroporation currents. For the −350 mV shock pulse, we do not know what percentage of the resistive current passes through the K^+ channels. For the worst situation, let us assume all of the resistive currents pass through the K^+ channels (even though it is impossible). In this case, we still have similar results. In other words, a +350 mV shock pulse evoked a current passing though the K^+ channels at least 9 times larger than a −350 mV shock pulse would have evoked, therefore generating 9 times higher local Joule heating on these specific membrane proteins. Yet this +350 mV pulse only caused one-ninth of the reduction of channel activity.

This analysis clearly indicates that the post-shock reduction of the K^+ channel activity is not directly related to the high-intensity electric shock-induced transmembrane currents through the K^+ channel proteins. Furthermore, it is not related to the shock-induced local Joule heating on the K^+ channels.

In summary, our studies show that supramembrane potential shock pulse-induced reductions in the K^+ channel functions are not directly correlated to either the global transmembrane currents or the channel currents. Therefore, neither the global thermal effects (membrane Joule heating) caused by the huge transmembrane currents nor the local thermal effect (Joule heating on the K^+ channels) mediated by larger channel currents plays a significant role in damaging the channel proteins. In other words, these experimental results provide strong evidence that during an exposure to an intensive electric field, the field-induced supramembrane potential difference (magnitude and polarity) plays a dominant role in the level of protein damages. This supramembrane potential difference might cause electroconformational changes in the charged particles or equivalent dipole moments in the channel proteins, resulting in channel dysfunction. Recently, we have succeeded in measuring the field-induced reductions in the intramembrane charge movement currents (Chen et al., 1998, submitted for publication) and in predicting shock-medicated decrements in the limiting charge particles in the K^+ channel gating system (Chen et al., 1997, submitted for publication).

It is necessary to point out that the magnitude of supramembrane potential differences that cause trivial thermal damages in channel proteins are studied only up to 500 mV. We do not rule out the possibility that when the field intensity further increases, the thermal effects may play a significantly more important role in damaging the membrane proteins.

This work was supported by National Institutes of Health Grant GM 50785 (to W.C.)

REFERENCES

Abramov, G. S., M. Bier, M. Capelli-Schellpfeffer, and R. C. Lee. 1996. Alteration in sensory nerve function following electric shock. *Burn*. 22:602–606.

Bischof, J. C., J. T. Padanilam, W. H. Holmes, R. M. Ezzell, R. C. Lee, E. G. Cravalho, R. G. Tompkins, M. L. Yarmush, and M. Toner. 1994. Dynamic of cell membrane permeability changes at supraphysiological temperatures. *Biophys. J.* 68:2608–2614.

Bommannan, D., L. Leung, J. Tamada, J. Sharifi, W. Abraham, and R. Potts. 1993. Transdermal delivery of luteinizing hormone releasing hormone: comparison between electroporation and iontophoresis in vitro. *Proc. Int. Symp. Control. Rel. Bioact. Mater.* 20:97.

Chang, D. C., P. Q. Gao, and B. L. Maxwell. 1991. High efficiency gene transfection by electroporation using a radio-frequency electric field. *Biochim. Biophys. Acta.* 1992:153–160.

Chen, W., and R. C. Lee. 1994a. An improved double Vaseline gap voltage clamp to study electroporated skeletal muscle fibers. *Biophys. J.* 66: 700–709.

Chen, W., and R. C. Lee. 1994b. Altered ion channel conductance and ionic selectivity induced by large imposed membrane potential pulse. *Biophys. J.* 67:603–612.

Chen, W., and R. C. Lee. 1994c. Electromediated permeabilization of frog skeletal muscle cell membrane: effect of voltage-gated ion channels. *Bioelectrochem. Bioenerg.* 34:157–167.

Chen, W., P. Li, and R. C. Lee. 1992. Efficacy of non-ionic surfactant for sealing electropermeabilized skeletal muscle fibers. *Biophys. J.* 61:2427.

Cole, K. S. 1972. Membrane, Ions and Impulses. University of California Press, Berkeley, CA. 569–590.

Cravalho, E. G., M. Toner, D. C. Gaylor, and R. C. Lee. 1992. Response of cells to supraphysiological temperatures: experimental measurements and kinetic models. *In* Electrical Trauma: The Pathophysiology, Manifestations, and Clinical Management. Cambridge University Press, London/New York. 281–300.

Ehrenberg, B., D. L. Farkas, E. N. Fluhler, Z. Lojewska, and L. M. Loew. 1987. Membrane potential induced by external electric field pulses can be followed with a potentiometric dye. *Biophys. J.* 51:833–837.

Hille, B. 1992. Ion Channels in Excitable Cell Membranes. Sinauer Associates, Inc., Sunderland, MA.

Hille, B., and D. T. Campbell. 1976. An improved Vaseline gap voltage clamp for skeletal muscle fibers. *J. Gen. Physiol.* 67:265–293.

Hui, C. S., and W. Chen. 1997. Charge movement in cut fibers of *Rana temporaria* containing 0.1 mM EGTA. *J. Physiol.*503:563–570.

Irving, M., J. Maylie, N. L. Sizto, and W. K. Chandler. 1987. Intrinsic optical and passive electrical properties of cut frog twitch fibers. *J. Gen. Physiol*. 89:1–40.

Jones, J. L., R. E. Jones, and G. Balasky. 1987. Microlesion formation in myocardial cells by high-intensity electric field stimulation. *Am. J. Physiol*. 253:H480–H486.

Kinosita, K., Jr., M. Hibino, H. Itoh, M. Shigemori, K. Hirano, Y. Kirino, and T. Hayakawa. 1992. Events of membrane electroporation visualized on a time scale from microsecond to seconds. *In* Guide to Electroporation and Electrofusion, D. C. Chang, B. M. Chassy, J. A. Saunders, and A. E. Sowers, editors. Academic Press, Inc., New York.

Kinosita, K., Jr., and T. Y. Tsong. 1977. Hemolysis of human erythrocytes by a transient electric field. *Proc. Natl. Acad. Sci. USA.* 74:1923–1927.

Kovacs, L., E. Rios, and M. F. Schneider. 1983. Measurement and modification of free calcium transients in frog skeletal muscle fibers by a metallochromic indicator dye. *J. Physiol.* 343:161–196.

Lau, C. P., and A. J. Camm. 1991. Rate-responsive pacing: technical and clinical aspects. *In* Cardiac Pacing and Electrophysiology, N. El-Sherif and P. Samet, editors. W. B. Saunders Co., Philadelphia. 524–544, 706–712.

Lee, R. C., D. G. Gaylor, D. L. Bhatt, and D. A. Israel. 1988. Role of cell membrane rupture in the pathogenesis of electrical trauma. *J. Surg. Res.* 44:709.

Lee, R. C., and M. S. Kolodney. 1987. Electrical injury mechanisms: electrical breakdown of cell membrane. *Plast. Reconstr. Surg.* 80: 672–679.

Mehrle, W., U. Zimmermann, and R. Hampp. 1985. Evidence for asymmetrical uptake of fluorescent dyes through electro-permeabilized membranes of Avena mesophyll protoplasts. *FEBS Lett*. 185:89–94.

Mir, L. M., S. Orlowski, J. Belehradek, and C. Paoletti. 1991. Electrochemotherapy: potentiation of antitumor effect of bleomycin by local electric pulses. *Eur. J. Cancer.* 27:68.

Okino, M., and H. Mohri. 1987. Effects of a high voltage electrical impulse and an anticancer drug on in vivo growing tumors, *Jpn. J. Cancer Res.* 78:1319.

O'Neill, R. J., and L. Tung. 1991. Cell-attached patch clamp study of the electropermeabilization of amphibian cardiac cells. *Biophys. J.* 59: 1028–1039.

Prausnitz, M. R., V. G. Bose, R. Langer, and J. C. Weaver. 1993. Electroporation of mammalian skin: a mechanism to enhance transdermal drug delivery. *Proc. Natl. Acad. Sci. USA*. 90:10504.

Raymond, E. I., A. S. L. Tang, D. W. Frazier, N. Shibata, P. S. Chen, and J. M. Wharton. 1991. Ventricular defibrillation: basic concepts. *In* Cardiac Pacing and Electrophysiology. N. El-Sherif and P. Samet, editors. W. B. Saunders Co., Philadelphia. 706–712.

Rouge, R. G., and A. R. Dimick. 1978. The treatment of electrical injury compared to burn injury: a review of pathophysiology and comparison of patient management protocols. *J. Trauma.* 18:43.

Sower, A. E., and M. R. Lieber. 1986. Electropore diameters, lifetimes, numbers, and locations in individual erythrocyte ghosts. *FEBS Lett*. 205:179–184.

Teissie, J., and M. P. Rols. 1994. Manipulation of cell cytoskeleton affects the lifetime of cell membrane electropermeabilization. *In* Electrical Injury: A Multidisciplinary Approach to Therapy, Prevention, and Rehabilitation. *Ann. N.Y. Acad. Sci.* 720:98–100.

Teissie, J., and T. Y. Tsong. 1980. Evidence of voltage-induced channel opening in Na/K ATPase of human erythrocyte membrane. *J. Membr. Biol*. 55:133–140.

Tovar, O., and L. Tung. 1992. Electroporation and recovery of cardiac cell membrane with rectangular voltage pulse. *Am. J. Physiol*. 92: H1128–H1136.

Tropea, B. I., and R. C. Lee. 1992. Thermal injury kinetics in electrical trauma. *J. Biomech. Eng.* 114:241–250.

Tsong, T. Y. 1991. Electroporation of cell membrane. *Biophys. J.* 60: 297–306.

Tsong, T. Y., and R. D. Astumian. 1986. Absorption and conversion of electric field energy by membrane-bounded ATPases. *Bioelectrochem. Bioenerg.* 15:457–476.

Tsong, T. Y., and R. D. Astumian. 1987. Electroconformational coupling and membrane protein function. *Prog. Biophys. Mol. Biol.* 50:1–45.

Winegar, R. A., J. W. Phillips, J. H. Yongblom, and W. F. Morgan. 1989. Cell electroporation is a highly efficient method for introducing restriction endonuclease into cells. *Mutat. Res*. 225:49–53.

Zimmermann, U., J. Vienken, and G. Pilwat. 1980. Development of drug carrier systems: electric field induced effects in cell membranes. *J. Electroanal. Chem*. 116:553–574.